
000 HYPERPARAMETER SEARCH ON THE TEST SET IN THE WILD

001

002

003 **Anonymous authors**

004 Paper under double-blind review

005 ABSTRACT

006

007 Systems neuroscience has rapidly adopted machine-learning techniques, but has yet to
008 develop a robust standardized methodology for assessing the performance of decoding
009 models. Methodological issues can sometimes be subtle, arising as a consequence of ex-
010 perimental design. Here, in contrast, we investigate the consequences of post-hoc model
011 selection: an issue which is neither subtle nor idiosyncratic. This occurs when a single test
012 set is used to both select hyperparameters and evaluate performance, which favors models
013 that overfit to ungeneralizable features of the test set. While the issues with this practice
014 have been well documented within the ML literature, it has seen continued use in several
015 domains, including systems neuroscience. To highlight this unfortunate practice, we per-
016 formed a series of experiments using a selection of models from affected EEG decoding
017 studies, finding that the overestimation of decoding accuracy in the affected studies was
018 substantial: ranging from 0.74–1.24%. Moreover, we demonstrate that post-hoc model
019 selection favors unstable model architectures, as the variability in their performance in-
020 creases the likelihood that an instance of the model will coincidentally match the test
021 set. Comparisons of model performance under post-hoc model selection may thus mis-
022 lead researchers into developing increasingly complex and unstable models which fail to
023 outperform simpler, more stable, ones.

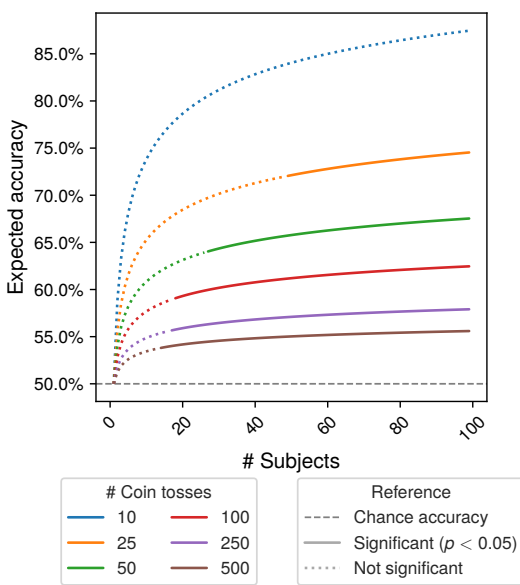
024

025 1 INTRODUCTION

026

027 In supervised machine-learning tasks, such as classification or regression, a model is trained on a training
028 set and then evaluated on a separate test set. However, when seeking a high-performing model, it is often
029 desirable to perform *model selection*, by considering a range of values for hyperparameters, such as the
030 learning rate, weight decay, or the number of training epochs. Model selection is generally performed by
031 using (a) validation set(s) to determine the most effective hyperparameters for a model, and then evaluating
032 the performance of a model trained with those hyperparameters on an independent test set. However, in
033 *post-hoc model selection*, there is no validation set, and instead, all models are evaluated on the same test
034 set, and the decoding accuracy is reported as the accuracy of the most performant model.

035 It may not be immediately obvious why this practice is problematic, as each model is evaluated on data not
036 used during training. However, as the number of models that are evaluated increases, the more likely it is that
037 the best-performing model has overfit to ungeneralizable features of the test set. By way of analogy, suppose
038 one wished to investigate the existence of precognitive abilities in humans by testing how often subjects can
039 correctly predict the outcome of a series of fair coin tosses. As Fig. 1 illustrates, the more subjects that are
040 tested, the more likely it is that one will randomly guess a high percentage of the outcomes correctly. If we
041 selected the subject with the most correct guesses and consider their performance in isolation, the evidence
042 for their precognitive abilities would appear compelling. However, the anomalous accuracy is simply a
043 consequence of sample size, and if the subject repeated the experiment, we would expect them to perform
044 at chance. The same principle applies to post-hoc model selection. As more models are evaluated, the
045 likelihood that the best-performing model has overfit to ungeneralizable features of the test set increases. In
046



fact, for given any classification task, and an arbitrarily high desired accuracy, a sufficiently large number of random models can always be found such that the expected accuracy of the best-performing model exceeds the desired accuracy. See the supplementary material for the corresponding proof of this property.

While the potential for post-hoc model selection to bias performance estimates is a well-known issue, its continued use can likely be attributed to the perception that the overestimation of decoding accuracy is negligible given a test set of sufficient size. Moreover, if the emphasis of a study is on demonstrating a relative improvement in decoding accuracy, then it might be thought that the relative performance of models is still meaningful, even if the absolute performance is overestimated. However, as our analysis will show, neither of these assumptions hold. In particular, we demonstrate that post-hoc model selection can result in an overestimation of decoding accuracy which is not only statistically significant, but also of considerable practical relevance. Furthermore, we show that it does not affect all models equally, but imparts a greater bias to unstable model architectures, as the variability in their performance increases the likely extent to which the best-performing instance of a model architecture has overfit to the test set. And since a primary goal of a decoding study is often to demonstrate the efficacy of a new feature-engineering technique or model architecture, the publication of results which favor unstable models may encourage the development of increasingly large, complex, and unstable models which do not necessarily outperform simpler models.

The prevalence of post-hoc model selection within systems neuroscience is difficult to establish. However, while investigating a separate methodological issue known as the *repeated-stimulus confound*, Kilgallen et al. (2025) observed that, of the 18 studies identified as vulnerable to the confound, 11 were found to evaluate decoding performance via post-hoc model selection (Bagchi & Bathula, 2021; 2022; Luo et al., 2023; Kalafatovich et al., 2020; 2023; Kalafatovich & Lee, 2021; Fares et al., 2020; Jiang et al., 2021; Xue et al., 2024; Ahmadieh et al., 2023; 2024). Moreover, two additional publications feature models which require some form of hyperparameter tuning, but describe no model-selection procedures (Zheng et al., 2020; Deng et al., 2023). Therefore, it is possible that post-hoc model selection was performed implicitly in these studies by repeating the experiments using different hyperparameter values until a satisfactory decoding accuracy was achieved.

094 **Table 1:** Models from affected studies included in our experiments, with reported accuracies.
 095

096 Publication	097 Model	100 Concept-decoding[*]	103 Stimulus-decoding[*]
098 Kalafatovich et al. (2020)	099 ADCNN	100 50.37% [†]	103 26.75%
100 Bagchi & Bathula (2021)	100 AW1DCNN	100 51.29% [†]	103 28.68%
101 Bagchi & Bathula (2022)	101 CT-Slim	101 51.96% [†]	103 26.08%
	102 CT-Fit	102 52.17% [†]	103 27.14%
	103 CT-Wide	103 52.33% [†]	103 29.44%
104 Deng et al. (2023)	104 RLSTM	104 52.69% ^{†‡}	104 29.92% [‡]
105 Kalafatovich et al. (2023)	105 TSCNN	105 54.28% [†]	105 —
106 Luo et al. (2023)	107 STST	107 54.82% [†]	107 29.98%

108 ^{**} The accuracy reported in the corresponding publication.

109 [†] Obtained under an evaluation procedure susceptible to the repeated-stimulus confound.

110 [‡] No model selection method was reported.

113 2 MATERIALS AND METHODS

115 2.1 DATA AND DECODING MODELS

116 To perform our experiments, we used the Stanford University dataset (SUD; Kaneshiro et al. 2015), as well
 117 as a selection of decoding models from studies previously identified by Kilgallen et al. (2025) as performing
 118 post-hoc model selection. However, the reproducibility of models from the affected publications was limited
 119 in several instances. We also elected to include the model from Deng et al. (2023), as it is possible that post-
 120 hoc model selection was performed implicitly in that study. The models selected for use in the experiments,
 121 and their reported accuracies, are detailed in Table 1.

122 To demonstrate that post-hoc model selection favors unstable models, we also performed an additional set
 123 of experiments using logistic regression. While introducing stochasticity during training can be a legitimate
 124 technique for improving model generalization, we decouple instability from training by injecting controlled
 125 noise only at evaluation time. Specifically, we train a standard logistic-regression model $z(x) = Wx + b$,
 126 which we refer to as the stable baseline. Then, at evaluation time, we sample randomized decisions using
 127 the Gumbel-Max trick (Gumbel, 1954; Huijben et al., 2022)

$$129 \hat{y} = \arg \max_k \{ z(x) + \beta (-\log(-\log U_k)) \} \quad U_k \stackrel{\text{iid}}{\sim} \text{Uniform}(0, 1) \quad (1)$$

130 where $\beta > 0$ controls the instability of the model’s predictions. By construction, as $\beta \rightarrow 0$, the procedure
 131 converges to the stable baseline, while an increase in β raises the probability that a different class is predicted.
 132 To reliably control instability, we use a fixed weight decay, as weight decay shrinks margins and thereby
 133 affects the probability that a different class will be predicted. Additionally, to ensure that our findings are
 134 relevant to real-world contexts, in all experiments, a separate model instance is trained for each value of β .
 135

136 2.2 MODEL TRAINING, SELECTION, AND EVALUATION PROCEDURES

138 To investigate the effects of post-hoc model selection in different contexts, we performed experiments for
 139 three distinct decoding tasks. Firstly, a 6-class concept-decoding task, where the objective is to predict
 140 the concept labels of responses to unseen stimuli. Secondly, the 6-class confounded concept-decoding task

Table 2: Accuracy by decoding task, model and selection method.

Model	Concept decoding		RSC Concept decoding		Stimulus decoding	
	Pre-hoc	Post-hoc	Pre-hoc	Post-hoc	Pre-hoc	Post-hoc
Affected models						
ADCNN	43.18	44.40	51.37	52.37	32.76	33.49
AW1DCNN	41.57	43.02	49.21	50.28	13.47	14.06
CT-Slim	40.99	42.34	48.75	49.99	22.60	23.30
CT-Fit	42.32	43.39	50.27	51.03	20.35	21.13
CT-Wide	42.52	43.56	50.53	51.27	20.50	21.33
RLSTM	40.76	41.95	47.91	48.77	18.81	19.37
TSCNN	41.38	42.76	48.44	49.61	24.75	25.52
STST	38.81	40.09	44.91	45.84	21.85	22.53
Additional models						
LR	37.74	38.01	43.96	44.36	12.98	13.12
Unstable-LR	37.56	38.38	43.87	44.64	12.93	13.36

performed in the affected publications, where the aim is to decode concept labels from unseen responses to previously seen stimuli. Lastly, a 72-class stimulus-decoding task, where the goal is to decode stimulus labels from unseen responses.

For all decoding tasks, we performed 12-fold nested cross validation with 11 inner folds. For each outer fold, one fold is used as the test set while the remaining 11 folds form the training set. The training set of each outer fold is then divided into 11 inner folds. Each inner fold is used as a validation set once while the remaining 10 inner folds form the training set. For each decoding task, we evaluated all hyperparameter combinations on both the inner and outer folds. Under post-hoc model selection, the hyperparameters which maximized accuracy on each outer fold were selected. And conversely, under pre-hoc model selection, the hyperparameters which maximized accuracy on the validation sets of each outer fold were selected. Details of the hyperparameter ranges used in our experiments are included in the supplementary material.

In our concept-decoding experiments, we extended the paired cross-validation procedure used in Kilgallen et al. (2025) to facilitate both pre-hoc and post-hoc model selection. This method had the added advantage of allowing us to quantify the bias imparted by post-hoc model selection both in isolation and in conjunction with the repeated-stimulus confound. See the supplementary materials for a pseudocode implementation of the cross-validation algorithm.

3 RESULTS

Table 2 presents the results of our decoding experiments. For each decoding task and model, we report the mean accuracy under both pre-hoc and post-hoc model selection. The concept-decoding and stimulus-decoding tasks were performed to investigate the impact of post-hoc model selection under two common decoding paradigms. As the affected publications we investigate in this work are also affected by the repeated-stimulus confound (RSC), the RSC concept-decoding task was performed to establish a comparison with the results reported in the affected publications. However, while we estimate the RSC concept-decoding accuracy of ADCNN as approximately 2% higher than was reported, the remaining models achieved accuracies below the reported values. The discrepancy was moderate for AW1DCNN, CT-Slim, CT-Fit, and CT-Wide (<2%), more severe for RLSTM and TSCNN (3–5%), but worst for STST ($\approx 9\%$).

188
189
190 **Table 3:** Selection bias by task and model.
191

Model	Concept decoding	RSC concept decoding	Stimulus decoding
Affected models			
ADCNN	1.22***	1.00***	0.73***
AW1DCNN	1.44***	1.06***	0.58***
CT-Slim	1.36***	1.24***	0.70***
CT-Fit	1.07***	0.76***	0.78***
CT-Wide	1.04***	0.74***	0.82***
RLSTM	1.19***	0.87***	0.56***
TSCNN	1.38***	1.17***	0.77***
STST	1.28***	0.93***	0.67***
Additional models			
LR	0.27***	0.39***	0.14*
Unstable-LR	0.81***	0.77***	0.43***

203 ‘*’, ‘**’, and ‘***’ indicate that the bias due to post-hoc model selection is greater than 0 at the $p < 0.05$,
204 $p < 0.01$, and $p < 0.001$ significance levels, respectively.
205
206

207 4 DISCUSSION

208

210 While it can be readily observed that accuracy is greater under post-hoc model selection than pre-hoc model
211 selection for all models and tasks, further analysis is required to assess the significance of the observed bias.
212

213 4.1 POST-HOC MODEL SELECTION OVERESTIMATES DECODING ACCURACY

214

215 One factor that may contribute to the continued use of post-hoc model selection is the perception that the
216 magnitude of the bias is relatively modest in practice. However, we empirically refute this rationale.
217

218 To support our claim, we performed hypothesis tests to determine if the bias affecting each model is signif-
219 icantly greater than zero, by applying one-tailed t-tests with confidence level $\alpha = 0.05$. At the task level,
220 to account for the separate hypothesis tests performed for each model, we applied the Holm-Bonferroni
221 procedure to adjust the significance levels of the tests (Holm, 1979). The results of the hypothesis tests are
222 presented in Table 3.

223 Our findings indicate that, for each task, the bias in decoding accuracy due to post-hoc model selection is
224 significantly different from zero for all models. Consequently, we conclude that selecting the hyperparameter
225 combination which results in the highest test-set accuracy results in an overestimation of decoding accuracy.
226 In fact, as Fig. 2 illustrates, the estimated accuracy of the model with the selected hyperparameters is not
227 just optimistic, it is generally overestimated by a greater margin than that of any other model. Moreover,
228 the substantial magnitude of the bias we observed indicates that it is not just statistically significant, but
229 of practical relevance. For instance, it can be observed from Table 1 that, for the confounded concept-
230 decoding task, the margin of improvement in each successive publication ranges from 0.36–1.59%, while
231 our corresponding estimates of bias range from 0.74–1.24%. This may explain why such a high-proportion
232 of studies which use the SUD also perform post-hoc model selection. In the absence of the bias conferred by
233 post-hoc model selection, the margin by which a model would need to outperform the current state-of-the-art
234 is effectively double the historical trend. Consequently, once a study which uses post-hoc model selection is
published, it is difficult for subsequent work to revert to a more robust practice.

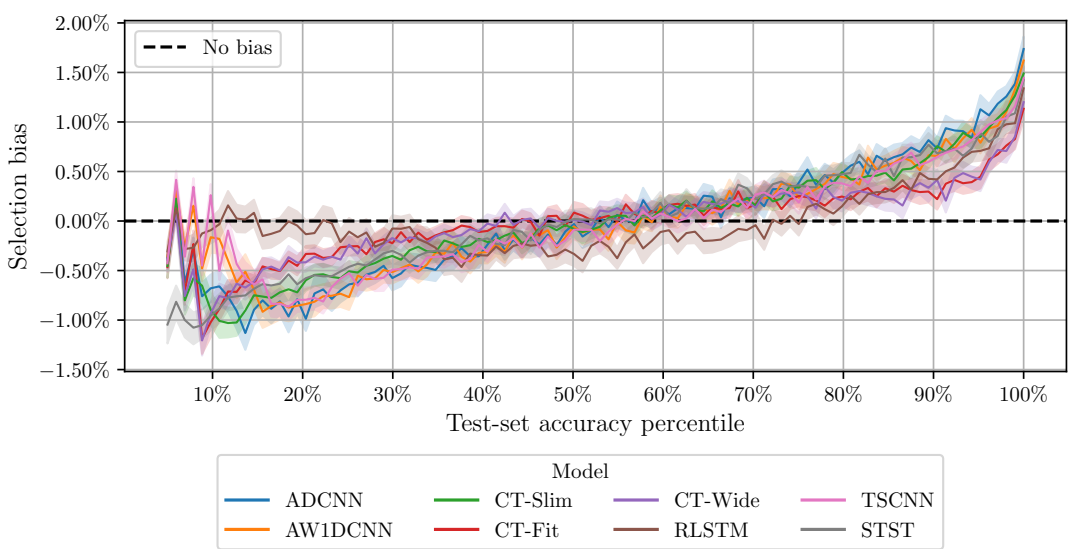


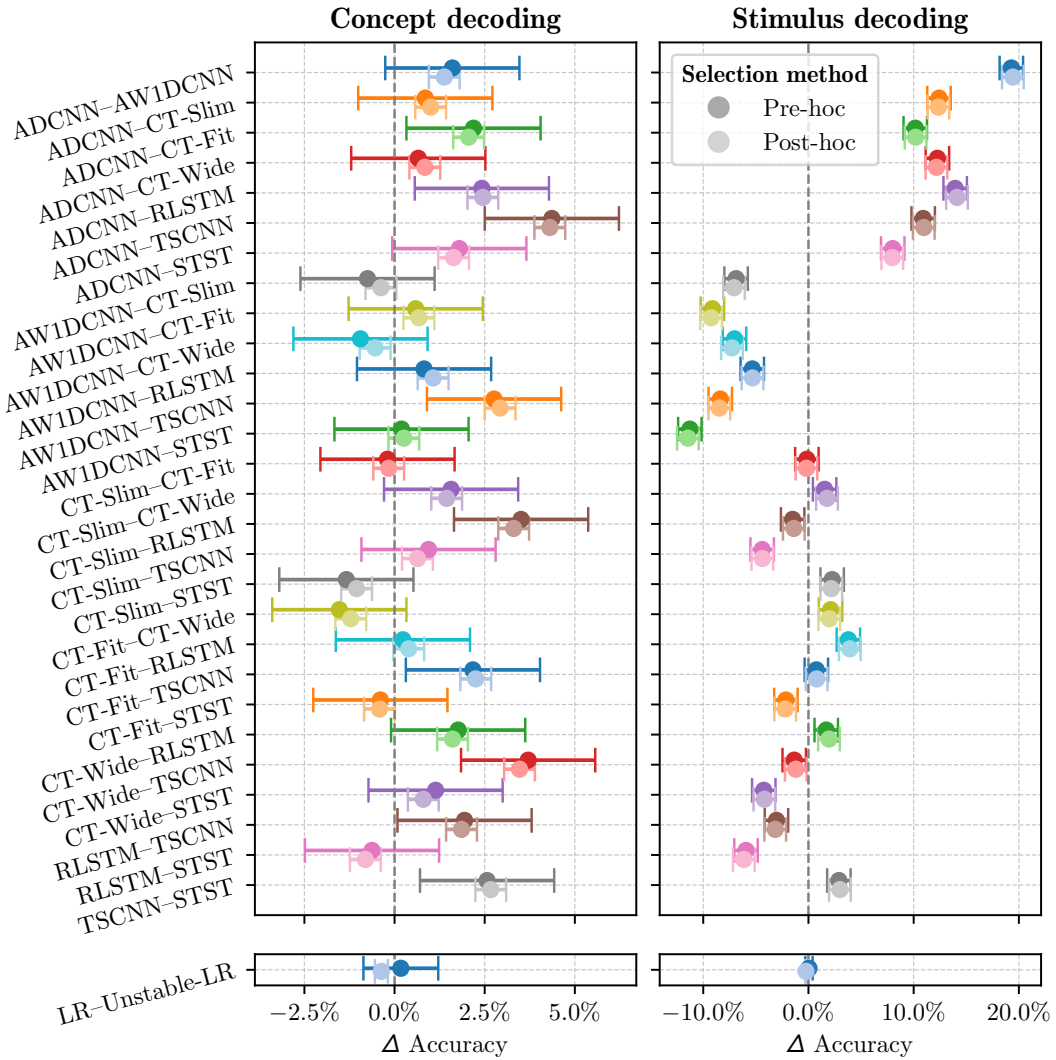
Figure 2: Hyperparameters selection on the test set is cherry-picking, just look at the rest of the fruit.
 For each model, subject, and fold in our concept-decoding experiments, we estimated the selection bias for the hyperparameter combination with the i th best accuracy on the test set by subtracting the test-set accuracy of the hyperparameter set with the i th best validation-set accuracy. It can be clearly seen that, for all models except RLSTM, the top 40–50% of all hyperparameter combinations overestimate accuracy. Moreover, the magnitude of the overestimation is proportional to the relative performance on the test set. Therefore, selecting model hyperparameters using the test set, is effectively cherry-picking the most optimistic, but least reliable, estimate of model performance.

4.2 POST-HOC MODEL SELECTION OVERESTIMATES THE SIGNIFICANCE OF INCREASES IN DECODING ACCURACY

Another potential explanation for the continued use of post-hoc model selection is the assumption that, despite any overestimation of accuracy, if it is standard practice, then relative improvements in performance are still meaningful across models or studies.

Therefore, to dispel any notions that two wrongs make a right, we demonstrate that, under post-hoc model selection, the apparent significance of relative improvements in accuracy is unreliable. To this end, for our concept-decoding and stimulus-decoding tasks, we fit a linear mixed-effects model to estimate the accuracy of each model. For both tasks, separate linear mixed-effects models were used to estimate accuracy under pre-hoc and post-hoc model selection. Subsequently, post-hoc analysis was used to estimate the contrast between different models using the Holm (1979) method. See the supplementary material for additional information on the linear mixed-effects model used to construct the confidence intervals.

Fig. 3 depicts the 95% confidence intervals of the contrasts for each task and model-selection method. With respect to the concept-decoding experiments, under post-hoc model selection, almost all contrasts are deemed statistically significant, while the more robust procedure would indicate otherwise. However, this finding was not duplicated in the stimulus-decoding experiments. We attribute this discrepancy to the nature of the decoding tasks. In our concept-decoding experiments, each test set is composed of responses to different unseen stimuli, while the test sets of the stimulus-decoding experiments all consist of responses to



317 **Figure 3: The illusion of progress.** For each pair of models, the 95% confidence interval for the relative
318 difference in decoding accuracy is depicted. An interval which does not include 0 indicates that the esti-
319 mate is different from zero with statistical significance. In our concept-decoding experiments, when model
320 hyperparameters are selected using a separate validation set, the difference in accuracy is statistically sig-
321 nificant for only 10/28 pairs of models. However, when hyperparameters are selected using the test set,
322 this increases to 26/28 pairs of models. Therefore, although each study claims that it establishes a new
323 state-of-the-art by outperforming prior solutions, the validity of this claim is questionable. However, in the
324 stimulus-decoding experiments, our hypothesis tests suggest that the only point of disagreement between
325 the two model-selection procedures is that LR–Unstable-LR is only statistically significant under post-hoc
326 model selection.

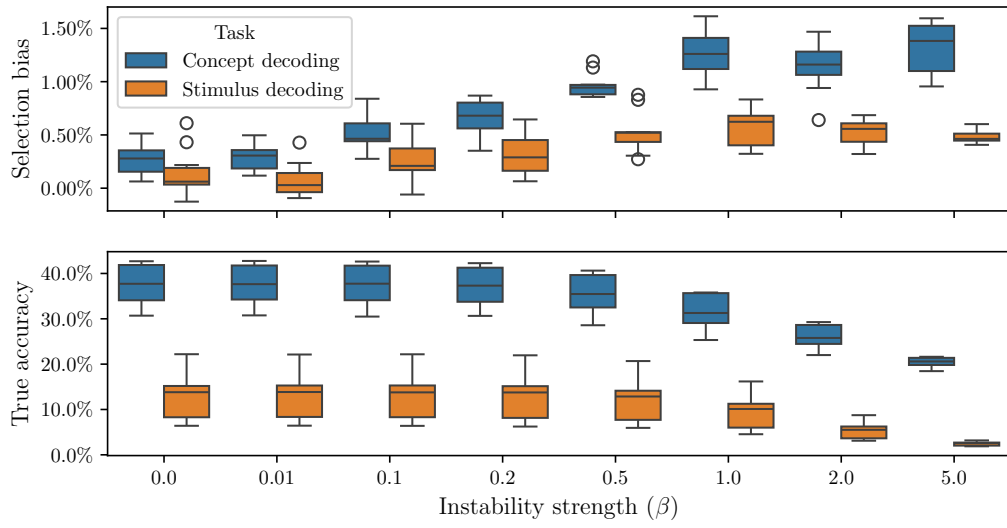


Figure 4: Why bother with veracity when volatility is king? The more unstable a model is, the less accurate it is, but the greater its accuracy is overestimated under post-hoc model selection. So, if a key aim of a decoding study is to achieve a new state-of-the-art, then the path of least resistance is to develop a less stable model of approximately equivalent decoding ability.

the same stimuli. Consequently, we observe that post-hoc model selection may be particularly brittle when a decoding task which is designed to capture the ability of a model to generalize to new stimuli.

4.3 POST-HOC MODEL SELECTION FAVORS UNSTABLE MODELS

The last potential motivation we offer for the continued use of post-hoc model selection is the belief that, regardless of its technical incorrectness it is a relatively harmless practice in the broader context of the literature. However, we present evidence which contradicts this hypothesis.

As mentioned previously, in addition to the models from publications known to perform post-hoc model selection, we also included two additional models, a conventional logistic-regression model, and a variant we designed to have controllably unstable predictions at evaluation time. It can be observed in Table 2 that, in all tasks, pre-hoc model selection favors conventional logistic regression, while the unstable variant is preferred under post-hoc model selection. Moreover, as Fig. 3 illustrates, post-hoc model suggestion suggests that our unstable logistic-regression model constitutes a statistically significant improvement over conventional logistic regression in both decoding tasks. However, as Fig. 4 illustrates, as instability increases, decoding accuracy decreases while selection bias increases.

The implications of this finding are far more insidious than it might appear. Model development is often an iterative process, where techniques like ablation studies are used to determine the aspects of a network which improve accuracy. However, since the overestimation of accuracy is proportionate to instability, this process may implicitly encourage researchers to develop increasingly complex and unstable models, which fail to outperform simpler solutions. Moreover, it is essentially a prerequisite of the publication process that a study documenting a novel decoding model should demonstrate that it outperforms prior solutions on some benchmark dataset. As a result, over time, the literature is likely to favor increasingly unstable models. While this may sound alarmist, it should be noted that the unstable logistic-regression model outperformed

376 its stable counterpart by a wider margin than RLSTM was reported to outperform CT-Wide (0.37% vs
377 0.36%).

379 Moreover, as novel decoding models may draw inspiration from prior solutions, the process as a whole may
380 encourage the proliferation of techniques which result in more volatile, but less reliable, models. In addition
381 to creating a misleading impression of progress, this issue may further contribute to the reproducibility crisis
382 within systems neuroscience, as the more volatile a model is, the more difficult it is to reproduce a specific
383 result. This may explain, in part, why the more recent a model is, the more our estimate of its performance
384 differs from the concept-decoding accuracy reported in the corresponding publication.

385 5 CONCLUSION

388 In this work, we investigated the consequences of post-hoc model selection, a well-known but underesti-
389 mated issue. We illustrated the theoretical nature of the problem using a thought experiment which high-
390 lighted that the same approach could also be used to support the existence of precognitive abilities in humans.

392 To demonstrate the severity of the issue in a real-world setting, we performed a series of decoding experi-
393 ments using a selection of models from affected publications. Our analysis of the results revealed that the
394 magnitude of the bias was both statistically significant and substantial for every model in all decoding tasks.
395 Subsequent analysis also revealed two more subtle issues with the procedure. Firstly, that it substantially
396 overestimates the significance of improvements in performance, and consequently creates a false impression
397 of rapid progress and the relative efficacy of different decoding techniques. And secondly, it preferentially
398 overestimates the accuracy of more unstable models, which may be implicitly encouraging researchers to
399 develop increasingly complex and unstable models, which fail to outperform simpler solutions.

400 Given the consistent and substantial bias we observed, as well as the severe and varied nature of the other
401 issues caused by post-hoc model selection, we suggest that its use should be immediately discontinued in
402 favor of more robust model-selection methods. Moreover, the publication of studies which employ a practice
403 known to be unsound indicates the need for both a more rigorous review process, and formal guidelines
404 regulating how the results of machine-learning experiments are reported.

405 AUTHOR CONTRIBUTIONS

406 Removed for blind review.

409 ACKNOWLEDGMENTS

411 Removed for blind review.

413 ETHICS STATEMENT

415 This work debunks EEG analysis work based on faulty methods. Exposing these incorrect methods and
416 consequent false results will allow resources wasted on continued use of these incorrect methods to be
417 reallocated. The debunked work also actively causes harm, including grant proposals rejected due to prelim-
418 inary results being uncompetitive with falsely-inflated performances based on faulty methods; manuscripts
419 rejected for the same reasons; time wasted attempting to replicate the debunked results; and students learning
420 invalid methods. Because the debunked work relates to brain-computer interfaces whose primary application
421 is helping people with disabilities (e.g., paralysis) interact with the world, the harm is not merely scientific
422 but also medical, with disproportionate affects on disabled people.

423 REPRODUCIBILITY STATEMENT

424

425 All data and code used to generate these results will be made publicly available following acceptance.

426

427 REFERENCES

428

429 Hajar Ahmadieh, Farnaz Gassemi, and Mohammad Hasan Moradi. A hybrid deep learning framework for
430 automated visual image classification using EEG signals. *Neural Computing and Applications*, 35(28):
431 20989–21005, October 2023.

432 Hajar Ahmadieh, Farnaz Gassemi, and Mohammad Hasan Moradi. Visual image reconstruction based on
433 EEG signals using a generative adversarial and deep fuzzy neural network. *Biomedical Signal Processing*
434 and Control, 87:105497, 2024. ISSN 1746-8094. doi: <https://doi.org/10.1016/j.bspc.2023.105497>. URL
435 <https://www.sciencedirect.com/science/article/pii/S1746809423009308>.

436 Subhranil Bagchi and Deepti R. Bathula. Adequately wide 1D CNN facilitates improved EEG based visual
437 object recognition. In *29th European Signal Processing Conference (EUSIPCO)*, pp. 1276–1280, Dublin,
438 Ireland, August 2021. IEEE.

439

440 Subhranil Bagchi and Deepti R. Bathula. EEG-ConvTransformer for single-trial EEG-based visual stimulus
441 classification. *Pattern Recognition*, 129:108757, September 2022.

442 Yaling Deng, Shuo Ding, Wenyi Li, Qiuxia Lai, and Lihong Cao. EEG-based visual stimuli classification
443 via reusable LSTM. *Biomedical Signal Processing and Control*, 82:104588, April 2023.

444 Ahmed Fares, Sheng-hua Zhong, and Jianmin Jiang. Brain-media: A dual conditioned and lateralization
445 supported GAN (DCLS-GAN): Towards visualization of image-evoked brain activities. In *Proceedings of*
446 *the 28th ACM International Conference on Multimedia*, pp. 1764–1772, Seattle WA USA, October 2020.
447 ACM.

448

449 Emil Julius Gumbel. *Statistical Theory of Extreme Values and Some Practical Applications: A Series of*
450 *Lectures*. Applied mathematics series. U.S. Government Printing Office, Washington, 1954.

451 Sture Holm. A simple sequentially rejective multiple test procedure. *Scandinavian Journal of Statistics*, 6
452 (2):65–70, 1979. ISSN 03036898, 14679469.

453

454 Iris A. M. Huijben, Wouter Kool, Max B. Paulus, and Ruud J. G. van Sloun. A review of the gumbel-max
455 trick and its extensions for discrete stochasticity in machine learning, 2022. URL <https://arxiv.org/abs/2110.01515>.

456

457 Jianmin Jiang, Ahmed Fares, and Sheng-Hua Zhong. A brain-media deep framework: Towards seeing
458 imaginations inside brains. *IEEE Transactions on Multimedia*, 23:1454–1465, 2021. doi: 10.1109/TMM.
459 2020.2999183.

460 Jenifer Kalafatovich and Minji Lee. Subject-independent object classification based on convolutional neural
461 network from EEG signals. In *9th International Winter Conference on Brain-Computer Interface (BCI)*,
462 pp. 1–4, Gangwon, South Korea, February 2021. IEEE.

463

464 Jenifer Kalafatovich, Minji Lee, and Seong-Whan Lee. Decoding visual recognition of objects from EEG
465 signals based on attention-driven convolutional neural network. In *IEEE International Conference on*
466 *Systems, Man, and Cybernetics (SMC)*, pp. 2985–2990, Toronto, ON, Canada, October 2020.

467 Jenifer Kalafatovich, Minji Lee, and Seong-Whan Lee. Learning spatiotemporal graph representations for
468 visual perception using EEG signals. *IEEE Transactions on Neural Systems and Rehabilitation Engineering*,
469 31:97–108, 2023.

470 Blair Kaneshiro, Marcos Perreau Guimaraes, Hyung-Suk Kim, Anthony M. Norcia, and Patrick Suppes. A
471 representational similarity analysis of the dynamics of object processing using single-trial EEG classifi-
472 cation. *PLOS ONE*, 10(8):e0135697, August 2015.

473
474 Jack A. Kilgallen, Barak A. Pearlmutter, and Jeffrey Mark Siskind. The repeated-stimulus confound in
475 electroencephalography, 2025. URL <https://arxiv.org/abs/2508.00531>.

476 Jie Luo, Weigang Cui, Song Xu, Lina Wang, Xiao Li, Xiaofeng Liao, and Yang Li. A dual-branch spatio-
477 temporal-spectral transformer feature fusion network for EEG-based visual recognition. *IEEE Transac-
478 tions on Industrial Informatics*, 20(2):1721–31, 2023.

479
480 Shuning Xue, Bu Jin, Jie Jiang, Longteng Guo, and Jing Liu. A hybrid local-global neural network for visual
481 classification using raw EEG signals. *Scientific Reports*, 14(1), November 2024. ISSN 2045-2322. doi:
482 [10.1038/s41598-024-77923-4](https://doi.org/10.1038/s41598-024-77923-4). URL <http://dx.doi.org/10.1038/s41598-024-77923-4>.

483 Xianglin Zheng, Zehong Cao, and Quan Bai. An evoked potential-guided deep learning brain representa-
484 tion for visual classification. In *International Conference on Neural Information Processing (ICONIP)*,
485 volume 1333, pp. 54–61. Springer International Publishing, Cham, 2020.

486

487

488

489

490

491

492

493

494

495

496

497

498

499

500

501

502

503

504

505

506

507

508

509

510

511

512

513

514

515

516

A.1 HOW POST-HOC MODEL SELECTION CAN BE USED TO ACHIEVE ARBITRARY ACCURACY

Theorem 1 Given any classification task, and an arbitrarily high desired accuracy, a sufficiently large number of random models can always be found such that the expected accuracy of the best-performing model exceeds the desired accuracy.

Proof 1 We begin by observing that, for any classification task, the accuracy of a random model on a test set of n samples follows some discrete probability distribution D over a finite uniform grid $G = \left\{ \frac{i}{n} \right\}_{i=0}^n$ on $[0, 1]$. Given a set of m independent random models, the expected accuracy of the best-performing model, A_m , is given by

$$A_m = \sum_{k=1}^n \frac{k}{n} \cdot \left[F\left(\frac{k}{n}\right)^m - F\left(\frac{k-1}{n}\right)^m \right] \quad (2)$$

where F is the cumulative distribution function (CDF) of D . And, since F is a CDF over $[0, 1]$, it holds that $F(x) \in [0, 1] \forall x \in [0, 1]$ and $F(x) = 1 \iff x = 1$. Therefore, it follows that, as m goes to infinity, $F(1)^m$ dominates the sum, and thus:

$$\lim_{m \rightarrow \infty} A_m = 1 \cdot \lim_{m \rightarrow \infty} F(1)^m = 1 \quad (3)$$

We can conclude from this that, for any $\epsilon > 0$, there exists $m \in \mathbb{N}$ such that $A_m > 1 - \epsilon$. Or equivalently, we can state that, for any classification task, under post-hoc model selection, evidence can always be found to suggest that a random model outperforms the state-of-the-art.

A.2 USING CLEVER CROSS VALIDATION TO QUANTIFY MODEL SELECTION BIAS

Algorithm 1 Construction of paired cross-validation folds for the concept-level experiments.

Input: stimulus-grouped folds $\{\mathbf{idx}_i^\alpha\}_{i=1}^S$ and stimulus-stratified folds $\{\mathbf{idx}_i^\beta\}_{i=1}^S$, of trials indexed by \mathbf{idx} , where S is the number of stimuli per category.

Output: Paired folds $\text{idx}_{i,j,\bullet}^\gamma$, for $i \in \{1, \dots, S\}$, $j \in \{1, \dots, S\} \setminus \{i\}$, and $\bullet \in \{\lambda, \alpha, \alpha', \beta, \beta'\}$.

640

```

for  $i \in \{1, \dots, S\}$  do
  for  $j \in \{1, \dots, S\} \setminus \{i\}$  do
     $\alpha_{i,j} \leftarrow \text{idx}_i^\alpha \cup \text{idx}_j^\alpha$ 
     $\beta_{i,j} \leftarrow \text{idx}_i^\beta \cup \text{idx}_j^\beta$ 
     $\text{idx}_{i,j,\alpha}^\gamma \leftarrow \text{idx}_i^\alpha \setminus \beta_{i,j}$ 
     $\text{idx}_{i,j,\alpha'}^\gamma \leftarrow \text{idx}_i^\alpha \setminus \beta_{i,j}$ 
     $\text{idx}_{i,j,\beta}^\gamma \leftarrow \text{idx}_i^\beta \setminus \alpha_{i,j}$ 
     $\text{idx}_{i,j,\beta'}^\gamma \leftarrow \text{idx}_j^\beta \setminus \alpha_{i,j}$ 
     $\text{idx}_{i,j,\lambda}^\gamma \leftarrow \text{idx} \setminus \alpha_{i,j} \cup \beta_{i,j}$ 
  end for

```

349

end for

561

Given a fold $\mathbf{idx}_{i,j}^\gamma$, the training set, stimulus-unconfounded test and validation sets, and stimulus-confounded test and validation sets are indexed by $\lambda, \alpha, \alpha', \beta$ and β' , respectively.

564 **Table 4:** Hyperparameter ranges used in the experiments.
 565

566 Model	567 Hyperparameter	568 Range	
569 ADCNN/AW1DCNN/RLSTM	learning rate	[0.0001]	
	weight decay	[0.0001, 0.001, 0.01, 0.1]	
	batch size	[64]	
	# training epochs	[1, 2, ..., 50]	
	CT-Fit/CT-Slim/CT-Wide	learning rate	[0.0001]
		weight decay	[0.0001, 0.001, 0.01, 0.1]
		γ	[0.5]
		batch size	[64]
		# training epochs	[1, 2, ..., 50]
570 TSCNN	Projection origin	Electrode 51 [†]	
	learning rate	[0.0001]	
	weight decay	[0.0001, 0.001, 0.01, 0.1]	
	batch size	[64]	
	# training epochs	[1, 2, ..., 50]	
	τ_d	0.2 [‡]	
	τ_f	0.8	
	571 STST	learning rate	[0.0001]
		weight decay	[0.0001, 0.001, 0.01, 0.1]
		batch size	[64]
		# training epochs	[1, 2, ..., 50]
		wavelet cmor($\Delta_f = 1.0$, $f_c = 1.0$)	
572 LR	learning rate	[0.0001]	
	weight decay	[0.0001]	
	batch size	[64]	
	# training epochs	[1, 2, ..., 100]	
	573 Unstable-LR	β	[0.01, 0.1, 0.2, 0.5, 1.0, 2.0, 5.0]
		learning rate	[0.0001]
		weight decay	[0.0001]
		batch size	[64]
		# training epochs	[1, 2, ..., 100]

596 ‘†’ The marked value uses 1-based indexing.
 597 ‘‡’ Relative to the distance from nasion to inion.

598 **A.3 HYPERPARAMETER SELECTION**

599 See Table 4.

600 **A.4 A POST-HOC ANALYSIS OF POST-HOC MODEL SELECTION**

601 The linear mixed-effects model used to estimate the contrasts depicted in Fig. 3 is described by

$$602 \quad Z_{i,j,k} = \beta_0 + \sum_{m=1}^M \beta_m \cdot M_i + s_j + \epsilon_{i,j,k} \quad s_j \sim \mathcal{N}(0, \sigma_s^2) \quad \epsilon_{i,j} \sim \mathcal{N}(0, \sigma^2) \quad (4)$$

603 where $Z_{i,j,k}$ denotes the decoding accuracy of the i th model, on the k th fold of the j th subject. The intercept
 604 is given by β_0 , and β_m is the fixed effect for the m th decoding model. We use M as a dummy variable for

611 decoding model, such that M_x is equal to 1 if $i = x$, and 0 otherwise. The residual error and the random
612 effect for the subject variable are denoted by ϵ and s respectively. While the mixed-effects model technically
613 only estimates the accuracy of each decoding model, post-hoc analysis was used to determine if any contrasts
614 were significantly different from zero.

615

616

617

618

619

620

621

622

623

624

625

626

627

628

629

630

631

632

633

634

635

636

637

638

639

640

641

642

643

644

645

646

647

648

649

650

651

652

653

654

655

656

657